

Performance of D-Bolts Under Dynamic Loading

Charlie C. Li · Chantale Doucet

Received: 11 July 2011 / Accepted: 14 November 2011 / Published online: 25 November 2011
© Springer-Verlag 2011

Abstract In this work, dynamic test results of D-bolts are presented. The rock bolt specimens studied are 20 and 22 mm in diameter and 0.8–1.5 m in section length. The bolts were tested at an impact velocity of 5.4–6.2 m/s and with impact energy varying from 10 to 60 kJ. In total, over 50 drop tests were conducted during a period of three years. The dynamic tests show that a D-bolt section of 22 mm × 1.5 m can sustain an impact of 56 kJ of a dynamic impact and absorb 60 kJ of energy prior to failure. The maximum impact energy of the 22 mm bolt is thus 37 kJ/m of bolt and the maximum energy absorption is 40 kJ/m. The displacement of the D-bolt increases linearly with the impact energy. A theoretical solution has been obtained for the relationship between the impact energy and the displacement of the bolt. It states that the energy absorption of a D-bolt section is proportionally related to the volume of the bolt section and the tensile strength and ultimate strain of the bolt material. It was also found that the magnitude of the impact energy determines whether or not the bolt fails, while the impact momentum determines how long the impact lasts. The impact duration increases linearly with momentum as long as the bolt shank does not fail.

Keywords Rock bolt · Energy-absorbing rock bolt · D-bolt · Dynamic test · Dynamic performance ·

Rock support · Ground support · Rock reinforcement · Laboratory test

1 Introduction

Rockburst is a serious concern for rock excavations in highly stressed rock masses. The occurrence of rockbursts is associated with stress changes after excavation. In accordance with the triggering mechanism, a rockburst event is classified as either *strain burst* or *fault-slip burst* (Li 2011a). Strain burst refers to a burst event that is directly related to stress concentration in the nearby field of an underground opening. After excavation, the tangential stresses in the superficial rock become elevated. In extreme cases, the stresses are so high that the rock is not capable of sustaining them. At this moment, the rock bursts out and the elastic energy stored in the rock is released in a violent manner. The excavation of underground openings may also result in reductions in the normal stresses on some pre-existing faults near the openings. This in turn brings about reductions in the shear resistance of the faults and slippage may occur along them. Such fault slippage induces strain/stress waves that propagate spherically outward from the place of slippage. This is called a seismic event in the mining industry. When the strain waves reach the walls and roof of the underground opening, a so-called fault-slip rockburst event may be triggered. A fault-slip rockburst is usually more powerful than a strain rockburst and typically cause more serious damages to underground infrastructures than a strain rockburst does. A number of studies on rockburst have been carried out in mining-active countries like Canada, South Africa and Australia in the past years. An example of such studies is the comprehensive Rockburst

C. C. Li (✉)
Department of Geology and Mineral Resources Engineering,
The Norwegian University of Science and Technology,
Trondheim, Norway
e-mail: charlie.c.li@ntnu.no

C. Doucet
CANMET Mining and Mineral Sciences Laboratories,
Natural Resources, Ottawa, Canada
e-mail: chantale.doucet@RNCAN-NRCAN.GC.CA

Research Program 1990–1995 (CAMIRO 1995). Among the subjects studied in the program, dynamic rock support is one that has been paid great attention.

In regard to rock support, a conventional support device performs one or more of the following three functions: reinforcement of the rock mass, retaining of broken rock and holding of the retaining devices (McCreath and Kaiser 1992). In the case of a rock bolt, its functions involve reinforcement of the rock and holding the retaining devices (plate, strap, meshes, shotcrete, etc.). In static and low-stress rock conditions, instabilities are mainly caused by gravitational rock falls. The principle of rock bolting in this case is that rock bolts must be strong enough to equilibrate the dead weight of the potentially falling block. Thus, the strength of the bolt is crucial for static rock support design. In dynamic loading conditions like rockburst, one deals with energy released from the rock rather than simply load or displacement. Either strain or fault-slip rockbursts will release a good amount of energy. The released energy of an ejected rock block is expressed as $\frac{1}{2}mv^2$; where, m is the mass of the ejected block and v the ejection velocity. This amount of energy must be absorbed by the support devices in a support system in order to avoid rock ejection. The energy absorption of a support device is expressed as its average load multiplied by the displacement. In addition to the transfer of energy, the interaction between the ejected rock and the support devices also involves a transfer of momentum. The momentum of the ejected rock is expressed as mv . This amount of momentum must be fully transferred to the support devices involved if the ejection is to be avoided. The momentum of a support system is expressed as Pt where P is the support load and t the transfer time in accordance with Newton's second law. We then have an equilibrium $Pt = mv$. This relationship implies that a short transfer time will result in a high support load and vice versa. If a rigid support system is used, the momentum-transfer time will be short, and the support load has to be high to satisfy the momentum equilibrium. This could cause the support load to exceed the strength of the system, resulting in premature failure of the support devices. When a yield support system is used, however, it yields at a predefined load level and deforms to certain extents to absorb the kinetic energy and to safely transfer the momentum. A yield support system is composed of yield support devices. Yield support devices are needed in burst-prone rock conditions in order to avoid rock ejections. Taking into account both energy absorption and momentum transfer, all support devices for dynamic rock support must be not only deformable but also strong, that is, they must have a satisfactory energy-absorbing capacity.

Rock bolt is an important type of support device in a support system. Conventional rock bolts such as encapsulated rebar and Split Set absorb little energy because of their small deformation capacity (rebar) or their small load-bearing capacity (Split Set). As early as in the 1990s, it was already recognised that energy-absorbing rock bolts are needed to combat rockburst (Ortlepp 1992, 1994). The first type of energy-absorbing rock bolt used by the mining industry may be the cone bolt invented in South Africa (Jager 1992; Ortlepp and Stacey 1995). It consists of a smooth steel bar with a flattened conical flare forged onto one end. The smooth bar is coated with a thin layer of wax, so that it will be easily de-bonded from the grout under pull loading. The cone bolt was originally designed for use with cement grout, but was later modified for resin grout (Simser 2001). The major difference between the modified cone bolt (MCB) and the original one is that in the modified version a blade is added to the bolt end for the purpose of resin mixing. Durabar is another type of yielding rock bolt from South Africa. The anchor of Durabar is a crinkled section of the smooth bar. When the face plate is loaded, the anchor slips along the crinkled profile in the cement grout at a certain pull load. The Garford dynamic bolt is an Australian invention which consists of a solid steel bar, an anchor and a coarse-threaded steel sleeve at the end. This bolt is characterized by its engineered anchor which allows the bolt to stretch by a large amount when the rock dilates (Varden et al. 2008). Roofex is another type of yielding bolt that has a similar anchoring mechanism to the Garford bolt (Charette and Plouffe 2007). Details of the performance of the above-yielding rock bolts are given in Li (2011a). Yield-Lok (Wu and Oldsen 2010) was recently introduced on the market. The anchor of the bolt is pre-encapsulated in engineered polymer to build its yielding device. All above mentioned yielding rock bolts accommodate rock dilation and absorb energies via either ploughing of the anchor in the grout (cone bolt and Yield-Lok) or slippage of the bolt shank through the anchor/grout (Garford bolt, Roofex and Durabar). A common factor among them is that they are all two-point anchored in boreholes. Efforts were made to use fully bonded and de-bonded threadbars for dynamic rock support (Player et al. 2008). Differently from the other rock bolts described above, threadbars absorb energies by partially or fully mobilizing the strength and deformation capacities of the bolt steel.

The D-bolt is a new type of energy-absorbing rock bolt. It differs from the above-yielding rock bolts in structure. The D-bolt is made of a smooth steel bar with a limited number of anchors spaced along the length of the bar. The sections between anchors are designed to be approximately 1 m long. The bolt is fully encapsulated in a borehole with

either cement or resin grout. The anchors are firmly fixed in the grout, while the bar sections have very weak or no bonding to the grout because of the smooth surface. The bar sections elongate plastically to absorb energies when subjected to dynamic shocks. The bolt has a high energy absorption capacity. For instance, 22-mm bolts can absorb 40 kJ of kinetic energy per metre of bolt shank. Because of the layout of the multi-anchors, the bolt has a reliable anchoring mechanism. Failure of one section does not affect the other sections of the bolt. Li (2010, 2011b) presents more details of the layout and principle of the D-bolt. In the past 3 years, an extensive dynamic testing program was undertaken to examine the dynamic performance of the bolt. The major findings of the tests as well as relevant analyses are presented in this paper.

2 Test Arrangement

2.1 Specimen Preparation

The bolt specimens are 20 and 22 mm in diameter and 1.8–2.1 m long (see Fig. 1). Each bolt specimen has three anchors plus threads and plate. Each anchor is composed of two ovals made on the bolt shank. The test section of the bolt is located between anchors 1 and 2. The length of the test section is defined as the centre–centre distance between the two adjacent anchor positions, while the effective stretch length is defined as the portion of the section that is subjected to stretching. The stretch length is equal to the length of the test section minus one anchor length (Fig. 1). The lengths of the test sections of the specimens tested were 0.8, 0.9 and 1.5 m. Their corresponding stretch lengths were 0.7, 0.8 and 1.4 m, respectively (every anchor is approximately 0.1 m long).

In the tests, boreholes were simulated with a split steel tube (see Fig. 2b). The tube has an inner diameter (ID) of 31.7 mm for the 20-mm bolts and 34.5 mm for the 22-mm bolts. The wall thickness of the tubes is 12 mm. The inner wall of the tube has a slightly spiral groove which gives the hole a rough surface in order to increase the bonding

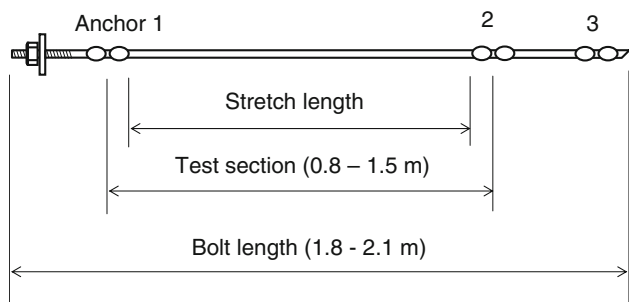


Fig. 1 Sketch of the bolt specimen

between the resin and the steel tube. Resin cartridges 28 mm in diameter were slid to the end of the tube. The bolt was inserted in the chuck of a drill mounted on a sliding rail with an independent advance drive system. The bolt was spun into the tubes with a steady advancement and a rotation speed of up to 375 RPM. Once the bolt reached the far end of the tube, the advance was stopped and the bolt was rotated for an additional 5 s. The tube split was located approximately in the middle of the test section of the bolt. The bolt specimen was fully encapsulated in the tube.

2.2 Testing Procedure

The tube-bolt specimen is suspended vertically by the upper end of the split tube. Each test consists of dropping a known mass from a known height onto a plate welded onto the lower portion of the split tube. The impact load is then transferred to the test section of the bolt through the resin and the anchor encapsulated in the lower portion of the tube. Figure 2 shows the test arrangement and the test rig. The tube-bolt specimen is inserted through the centre of the weight and an electromagnet is located above. The top of the tube is attached to the support frame of the test rig. The weight is magnetically attached to the electromagnet. The magnet and, in turn, the weight are lifted by a pair of cranes mounted on the top of the machine. By cutting off the power to the magnet, the weight falls freely onto the impact plate.

The instrumentation used consists of plate and end displacement monitors and load cells placed below the impact plate and below the bolt plate. Both the plate and the end displacements of the bolt are measured by linescan cameras. The plate displacement refers to the displacement

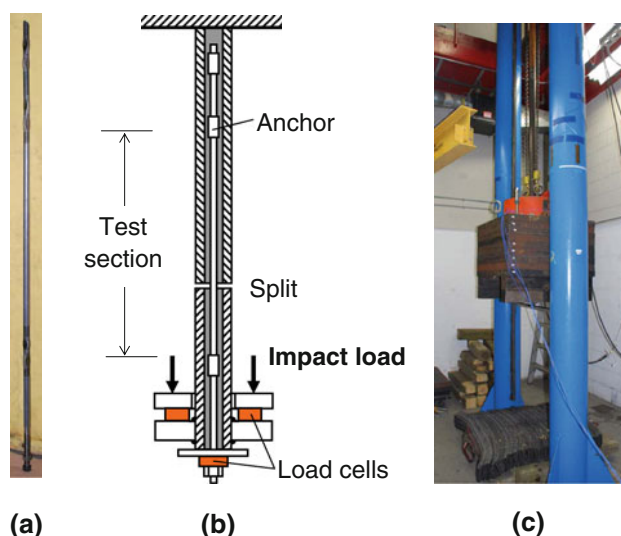


Fig. 2 a Bolt specimen, b test set up, c test rig

measured at the bolt plate, while the end displacement refers to the movement of the upper end of the bolt. The difference between the two displacements defines the displacement (i.e., elongation) of the test section. The load cells below the impact plate measure the impact load borne by the test section. The load cells below the bolt plate measure the load experienced by the bolt plate.

With a drop test, the total energy input is composed of two portions. The first portion is called impact energy which is defined as the maximum kinetic energy when the drop mass hits the target. Its magnitude is mgh where m is the drop mass, g the gravity acceleration and h the free-fall height. The second portion is an extra energy input induced during the elongation of the specimen, the magnitude of which is $mg\delta$ where δ stands for the elongation of the specimen.

3 Test Results

A number of rockburst events in deep metal mines in Canada and South Africa were studied in detail, using back-calculations among other methods. It was found that the maximum ejection velocity of ejected rock is in the range of 5–6 m/s (CAMIRO 1995). Higher ejection velocities up to 10 m/s were also reported in some cases, but they were the velocities of small rock pieces (Ortlepp 1992). In the dynamic drop tests presented in this paper, the impact velocity is in the range of 5–6 m/s.

Three series of dynamic tests were carried out at the CANMET Mining and Mineral Sciences Laboratory (CANMET-MMSL), Ottawa, Canada. In the first series, the bolt specimens were 20 mm in diameter with a 0.8-m-long test section. In the second and third series, the specimens were 22 mm in diameter and the test section lengths were 0.9 and 1.5 m, respectively.

When the test section is loaded, it elongates and the tube opens at the split. The test section fails when its deformation limit is reached. Figure 3 shows the final opening of the split tube, that is, the ultimate displacement of the test section. In this case, the specimen failed in the middle of the section. The dynamic performance of a bolt can be described by the curves of impact load versus displacement and versus impact

duration. Such curves of a few representative 22-mm specimens are presented in Figs. 4, 5, 6, 7. Figure 4 shows the curves of specimen D2-A2 with a 0.9-m-long test section. The specimen was tested with an impact of 30 kJ (drop mass = 2,006 kg and drop height = 1.5 m). Because of the vertical loading manner of the drop test, an extra energy input is added to the testing system during the elongation of the bolt section. Thus, the total energy input should be the sum of the impact energy and the extra energy input. However, as this second energy is due to the reaction of the bolt to the impact and that different bolts react in very different manners to dynamic impacts, it is best to analyse and compare bolts using the impact energy. This energy value should also be the one used for design purposes. Therefore, only the impact energy is used in presenting the test results in this section. When subjected to dynamic loading, the test section deformed elastically from A to B (Fig. 4). It yielded at B and then elongated at the yielding and hardening levels until the kinetic energy was used up at C. The section elongated by about 110 mm without failure. Afterwards, the mass rebounded upward, and the load in the section dropped to zero at D. The duration from the start of impact (A) to the beginning of rebound (C) is defined as the impact duration. The impact duration of specimen D2-A2 is 46 ms.

Specimen M6 has dimensions of 22 mm \times 1.5 m (diameter \times section length). It was tested with an impact of 50 kJ (drop mass = 2,897 kg and drop height = 1.76 m; see Fig. 5). The loading process of this specimen is similar to that of the previous one, but it elongated more because of its longer test section (1.5 m) and the higher impact energy. The test section elongated by about 200 mm without the failure. The load transferred to the bolt plate is also plotted in the load–displacement diagram shown in Fig. 5a. The plate load is less than half of the ultimate load in the bolt shank. This means that the bolt anchor effectively reduces the load transferred to the bolt plate. The impact lasted 62 ms for this specimen, as shown in Fig. 5b.

Specimen M5 also has dimensions of 22 mm \times 1.5 m. It was tested with an impact of 56 kJ (drop mass = 2,897 kg and drop height = 1.97 m). The specimen elongated by about 220 mm before failing (see Fig. 6a). The plate load of this specimen is less than one-third of

Fig. 3 The ultimate plastic displacement of a specimen of 22 mm \times 1.5 m after dynamic testing with impact energy of 56 kJ



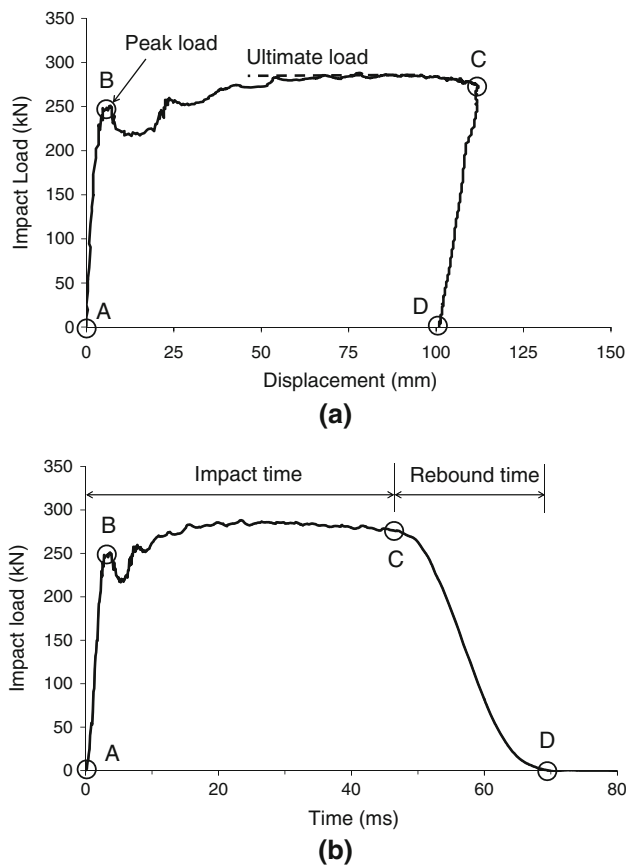


Fig. 4 Dynamic test results of specimen D2-A2 (22 mm × 0.8 m) tested with impact energy of 30 kJ and a momentum of 11 kN s without failure. **a** Impact load versus displacement, **b** impact load versus time

the ultimate load in the bolt shank. The impact lasted 64 ms for this specimen, as shown in Fig. 6b.

Specimen M2 was tested with an impact of 20 kJ. The specimen did not fail until the fourth drop, as displayed in Fig. 7. In the first drop, the elongation and impact duration are higher, 72 mm and 32 ms, respectively, than in the subsequent two drops. This difference may be explained by the hardening effect of the material after the first drop. Drops 2 and 3 have similar displacements and impact durations, approximately 63 mm and 25 ms, respectively. The dashed line in Fig. 7a marks the yield/hardening loads of the four drops. This envelope is similar to the complete load–displacement curve of a specimen impacted at a higher energy in one drop, such as M5.

The results of the dynamic tests and their input parameters are summarised in Table 1. The input parameters include the drop mass and height as well as the corresponding impact velocity, momentum and kinetic impact energy. The test results are the displacement and impact duration of the test section.

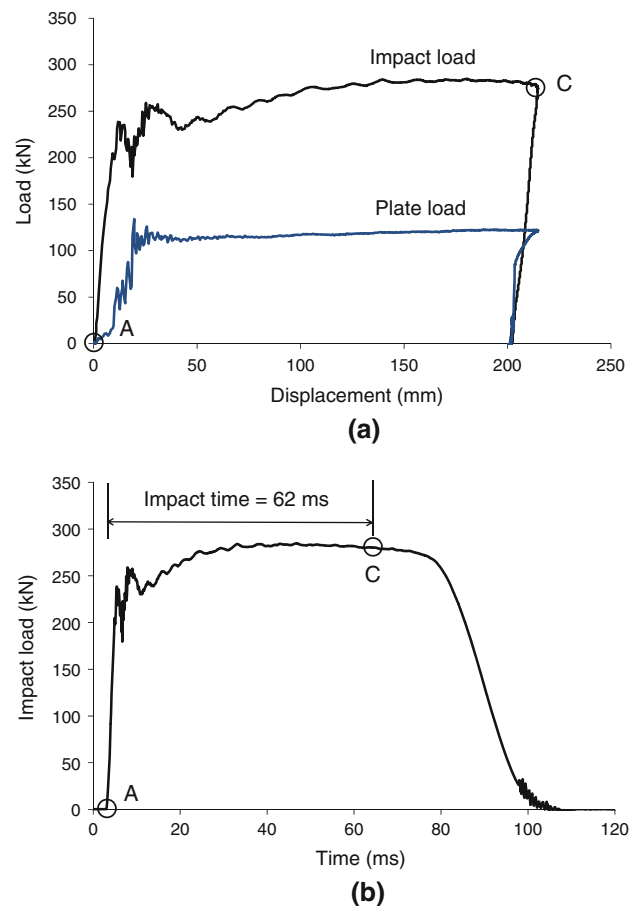


Fig. 5 Dynamic test results of specimen M6 (22 mm × 1.5 m) tested with impact energy of 50 kJ and a momentum of 17 kN s without failure. **a** Impact load versus displacement, **b** impact load versus time

4 Analysis

4.1 Discussion of the Test Results

Specimen M6 was dynamically loaded by an impact of 50 kJ without the failure, while specimen M5 failed with impact energy of 56 kJ. The curves in Figs. 5, 6 represent the dynamic responses of the D-bolt when subjected to large-magnitude seismic events. Specimen M2 was tested with a smaller impact energy (20 kJ) than M5 and M6. Therefore, the curves in Fig. 7 represent the dynamic responses of the D-bolt when subjected to a number of small-magnitude seismic events. Comparing the load–displacement curves in Figs. 5, 6, 7, it is seen that the yield, hardening and ultimate loads of the specimens are similar regardless of the magnitude of the impact energy as long as the impact results in plastic deformation in the bolt shank. However, the ultimate displacement of the multi-impact specimen (M2) is 10–20% larger than that of the other two

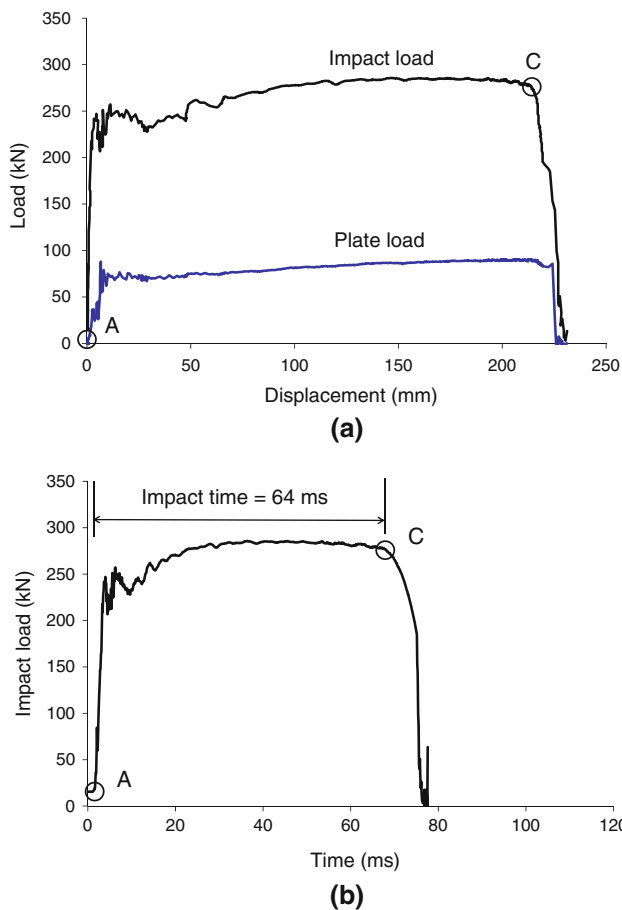


Fig. 6 Dynamic test results of specimen M5 (22 mm × 1.5 m) tested with impact energy of 56 kJ and a momentum of 18 kN s. The specimen failed. **a** Impact load versus displacement, **b** impact load versus time

single-impact specimens. This difference indicates that the bolt may be able to absorb slightly more energy when it is subjected to a number of small seismic events than when it is subjected to a single- and large-seismic event possibly because of the strain-hardening effect of the impacts on the steel.

The peak impact load is approximately at the same level as the ultimate impact load when the bolt is subjected to its first impact (see Figs. 4, 5, 6 and the first drop in Fig. 7). The peak load becomes slightly higher than the ultimate load in the subsequent drops (see drops 2 and 3 in Fig. 7). The increase in the peak load is attributed to hardening of the material as it is repeatedly subjected to dynamic impacts.

In ground support design, the bolt plate is important in establishing a link between the bolt and surface supports, such as mesh or shotcrete. As ground support works as a whole, it will only be as strong as its weakest link. It is therefore very important to maintain that link between the bolt and the surface support so that the load can be properly

transferred. Preventing the plate from overloading can help to protect the support system from damage. For the D-bolt, an anchor is placed close to the bolt threads and the plate. Figures 5, 6 show that the plate load is significantly smaller than the bolt shank load. The other tests show the same tendency; that is, the plate load is only 20–40% of the shank load, which means that the D-bolt can prevent premature failure of the bolt plate as long as all of its anchors are encapsulated in the grout.

4.2 Impact Energy and Displacement

Most of the impact energy is consumed for plastic deformation of the test section with a very small portion being transformed to elastic energy stored in the testing facility. In addition to the free-fall impact energy, a small amount of extra energy is put into the testing system due to the elongation of the test section. The input and dissipated output energies, therefore, are in equilibrium as follows:

$$W_{in} + mg\delta = P\delta + W_e \quad (1)$$

or,

$$\delta = \frac{W_{in} - W_e}{P - mg}, \quad (2)$$

where, W_{in} stands for the impact input energy, m the drop mass, P the average impact load, δ the plastic elongation (or displacement) of the bolt section and W_e the elastic energy stored in the testing facility.

The test results of the 22 mm × 1.5 m specimens are presented in Fig. 8. The triangles in the figure represent the displacements of the specimens after drops without the failure. The displacement increases approximately linearly with the impact energy. The solid line is the theoretical solution of the impact energy–displacement relationship in accordance to (2) by setting $P = 276$ kN (the corresponding average tensile strength is $\sigma_a = 726$ MPa) and $W_e = 1.5$ kJ. The theoretical solution agrees well with the test results. The ultimate displacements of four specimens are also plotted as diamonds in the diagram. The ultimate displacement tends to decline slightly with an increase in the impact energy. The intersection of the ascending solid line of the displacement per drop and the descending dashed line of the ultimate displacement marks the maximum impact energy that the bolt section can sustain. It is obtained that the maximum impact energy of the 22 mm × 1.5 m bolt section is 56 kJ, corresponding to 37 kJ per metre of bolt. As said previously, the bolt absorbs more than the impact energy because of the extra energy input related to shank elongation. A diagram similar to Fig. 8 can be constructed for the displacement versus the total input energy (i.e., the impact energy + the extra energy). It is obtained in such a diagram that the

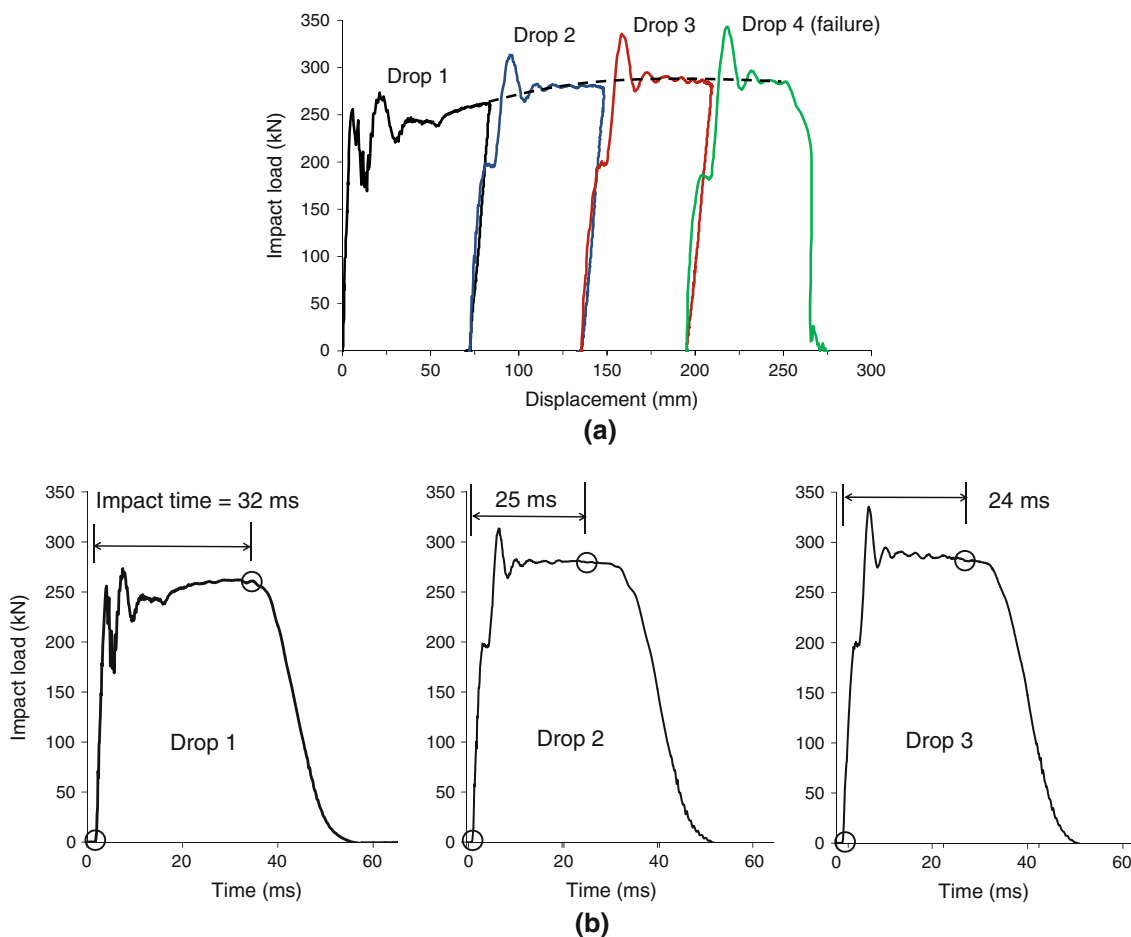


Fig. 7 Dynamic test results of specimen M2 (22 mm × 1.5 m) tested with impact energy of 20 kJ and a momentum of 7.3 kN s. **a** Impact load versus displacement, **b** impact load versus time

22 mm × 1.5 m bolt section can absorb 60 kJ of energy prior to the failure, which corresponds to 40 kJ per metre of the bolt shank.

The energy dissipated for plastic deformation of the section can be expressed as:

$$W_p = P\delta = \sigma_a \varepsilon AL$$

where, σ_a is the average dynamic tensile strength of the bolt material, ε the plastic strain, A the area of the cross section of the bolt shank and L the length of the test section. The maximum energy absorption of the section is thus expressed as:

$$W_{p,max} = \sigma_a \varepsilon_{ult} AL \tag{3}$$

where, ε_{ult} is the ultimate strain of the bolt steel. Expression (3) means that the energy absorption of a bolt section is equal to the plastic energy density ($\sigma_a \varepsilon_{ult}$) times the volume of the bolt section (AL).

4.3 Impact Momentum and Impact Duration

The drop test is essentially a collision between the drop mass and the stretch section of the bolt. In accordance with Newton’s second law, the momentum of a mass is equal to the product of the collision force and the impact duration, that is:

$$mv = Pt \tag{4}$$

where, m stands for the drop mass, v the velocity of the mass, P the average collision force and t the impact duration. Thus, the impact duration can be expressed as:

$$t = \frac{mv}{P} = \frac{M}{P} \tag{5}$$

or,

$$t = \frac{1}{\sigma_a} \frac{M}{A} \tag{6}$$

Table 1 Drop test results of D-bolts

| Spec. no. | Test section (dia. × length) (mm) | Drop no. | Input parameters | | | Output | | | Total input energy (kJ) | Failure (no/yes) |
|-----------|---|----------|-------------------|--------------------------|-------------------|--------------------------------|-------------------------|----------------|----------------------------|---------------------|
| | | | Drop mass (kg) | Impact velocity (m/s) | Moment. (kN s) | Impact energy (kJ) | Impact duration (ms) | Displ. (mm) | | |
| D1-1 | 20 × 800 | 1 | 893 | 5.4 | 4.8 | 13 | 27 | 52 | 13.6 | No |
| | | 2 | 893 | 5.4 | 4.8 | 13 | 22 | 48 | 13.6 | No |
| | | 3 | 893 | 5.4 | 4.8 | 13 | 10 | 41 | 10.1 | Yes |
| D1-2 | 20 × 800 | 1 | 893 | 5.4 | 4.8 | 13 | | 50 | 13.6 | No |
| | | 2 | 893 | 5.4 | 4.8 | 13 | | 48 | 13.6 | No |
| | | 3 | 893 | 5.4 | 4.8 | 13 | | 45 | 11.8 | Yes |
| D1-3 | 20 × 800 | 1 | 893 | 5.4 | 4.8 | 13 | | 57 | 13.6 | No |
| | | 2 | 893 | 5.4 | 4.8 | 13 | | 48 | 13.6 | No |
| | | 3 | 893 | 5.4 | 4.8 | 13 | | 35 | 8.9 | Yes |
| D1-5 | 20 × 800 | 1 | 893 | 5.4 | 4.8 | 13 | | 53 | 13.6 | No |
| | | 2 | 893 | 5.4 | 4.8 | 13 | | 49 | 13.6 | No |
| | | 3 | 893 | 5.4 | 4.8 | 13 | | 11 | 6.0 | Yes |
| L6 | 20 × 1,500 | 1 | 1,338 | 5.4 | 7.3 | 20 | 33 | 82 | 20.8 | No |
| | | 2 | 670 | 5.4 | 3.6 | 10 | 13 | 40 | 10.1 | No |
| | | 3 | 670 | 5.4 | 3.6 | 10 | 15 | 41 | 10.1 | No |
| | | 4 | 670 | 5.4 | 3.6 | 10 | 14 | 41 | 10.1 | No |
| | | 5 | 670 | 5.4 | 3.6 | 10 | 14 | 40 | 10.1 | No |
| | | 6 | 670 | 5.4 | 3.6 | 10 | 12 | 43 | 10.0 | Yes |
| L3 | 20 × 1,500 | 1 | 2,674 | 5.4 | 14.5 | 39 | 63 | 178 | 44.0 | No |
| L4 | 20 × 1,500 | 1 | 2,674 | 5.4 | 14.5 | 39 | 62 | 181 | 44.1 | No |
| L5 | 20 × 1,500 | 1 | 2,674 | 5.4 | 14.5 | 39 | 64 | 178 | 44.0 | No |
| L2 | 20 × 1,500 | 1 | 2,897 | 5.4 | 15.7 | 43 | 61 | 218 | 46.2 | Yes |
| Spec. no. | Test section (dia. × length) (mm) | Drop no. | Input parameters | | | Output | | | Total input energy (kJ) | Failure (no/yes) |
| | | | Drop mass (kg) | Impact velocity (m/s) | Moment. (kN s) | Free-fall input energy (kJ) | Impact duration (ms) | Displ. (mm) | | |
| D2-A2 | 22 × 900 | 1 | 2,006 | 5.4 | 10.9 | 30 | 46 | 101 | 31.5 | No |
| D2-A4 | 22 × 900 | 1 | 2,229 | 5.4 | 12.1 | 33 | 43 | 108 | 35.2 | No |
| D2-A6 | 22 × 900 | 1 | 2,452 | 5.4 | 13.3 | 36 | 46 | 143 | 36.5 | Yes |
| D2-A3 | 22 × 900 | 1 | 2,675 | 5.4 | 14.5 | 39 | 35 | 142 | 36.9 | Yes |
| M2 | 22 × 1,500 | 1 | 1,338 | 5.4 | 7.3 | 20 | 32 | 72 | 20.6 | No |
| | | 2 | 1,338 | 5.4 | 7.3 | 20 | 25 | 65 | 20.5 | No |
| | | 3 | 1,338 | 5.4 | 7.3 | 20 | 24 | 62 | 20.5 | No |
| | | 4 | 1,338 | 5.4 | 7.3 | 20 | | 35 | 18.0 | Yes |

Table 1 continued

| Spec. no. | Test section (dia. × length) (mm) | Drop no. | Input parameters | | | Output | | | Total input energy (kJ) | Extra input energy (kJ) | Total input energy (kJ) | Failure (no/yes) |
|-----------|-----------------------------------|----------|------------------|-----------------------|----------------|-----------------------------|----------------------|-------------|-------------------------|-------------------------|-------------------------|------------------|
| | | | Drop mass (kg) | Impact velocity (m/s) | Moment. (kN s) | Free-fall input energy (kJ) | Impact duration (ms) | Displ. (mm) | | | | |
| M3 | 22 × 1,500 | 1 | 2,897 | 5.4 | 15.7 | 43 | 61 | 167 | 4.7 | 47.4 | No | |
| M6 | 22 × 1,500 | 1 | 2,897 | 5.9 | 17.0 | 50 | 62 | 192 | 5.5 | 55.5 | No | |
| M7 | 22 × 1,500 | 1 | 2,897 | 5.9 | 17.0 | 50 | 65 | 196 | 5.6 | 55.6 | No | |
| M8 | 22 × 1,500 | 1 | 2,897 | 5.9 | 17.0 | 50 | 64 | 198 | 5.6 | 55.6 | No | |
| M5 | 22 × 1,500 | 1 | 2,897 | 6.2 | 18.0 | 56 | 64 | 226 | 6.4 | 60.0 | Yes | |
| M4 | 22 × 1,500 | 1 | 2,897 | 6.4 | 18.6 | 60 | 60 | 225 | 6.4 | 63.6 | Yes | |

The drop height of all the specimens except M4–M7 is 1.76 m for M6 and M7, 1.97 m for M5 and 2.1 m for M4. The total input energy is the sum of the free-fall impact energy and the extra energy due to specimen elongation for specimens that are not failed. For specimens that are failed, the total input energy is obtained by integrating the load–displacement curve

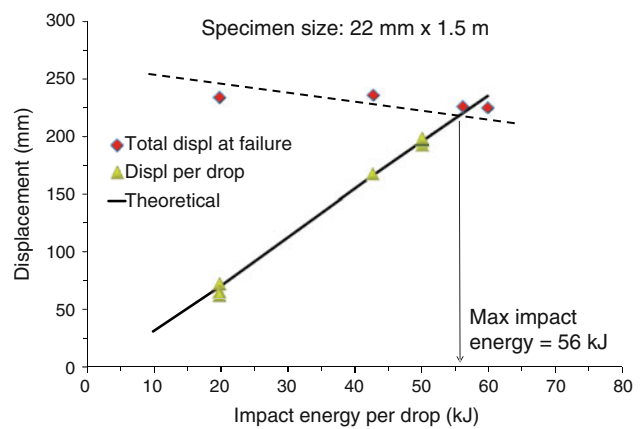


Fig. 8 Displacement versus impact energy for 22 mm × 1.5 m specimens

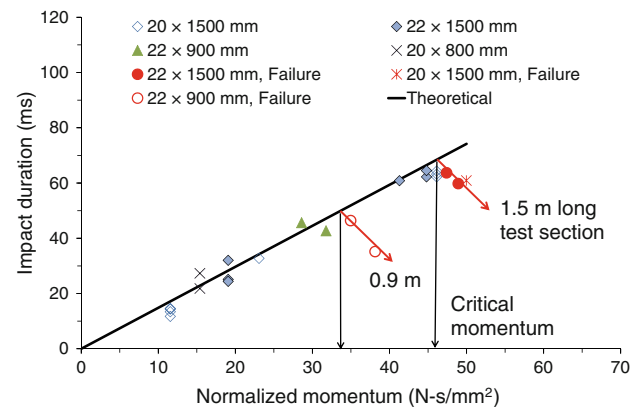


Fig. 9 Impact duration versus normalised impact momentum for bolt specimens of different lengths and diameters

where, M is the impact momentum, (M/A) stands for the normalised momentum per unit cross-sectional area of the bolt shank.

The impact durations of all specimens are scatter plotted versus the normalised impact momentum in Fig. 9. Substituting the average dynamic tensile strength of the steel, $\sigma_a = 726$ MPa, into (6) yields a theoretical expression for the relationship between the impact duration, t , and the normalised impact momentum, M/A :

$$t = 1.38 \times \frac{M}{A} \tag{7}$$

where, the impact duration t is expressed in ms and the normalised momentum M/A is in $N\ s/mm^2$. The theoretical solution, represented by the solid line in Fig. 9, agrees very well with the test results. In general, the impact duration increases linearly with the impact momentum as long as the specimen does not fail. Five specimens failed in the tests. It is seen in the figure that the impact duration of the failed specimens decreases approximately linearly with an

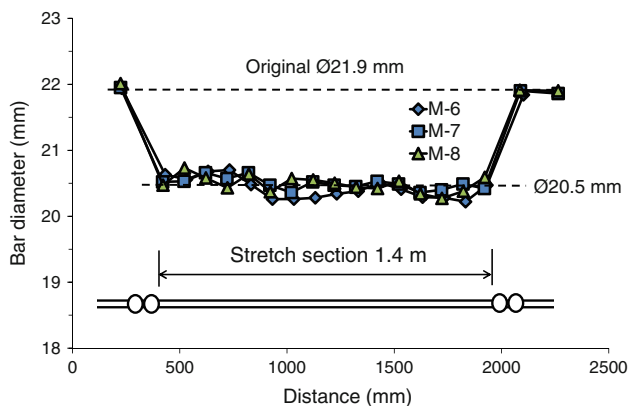


Fig. 10 Diameter reduction in the test section after impact testing with impact energy 50 kJ for three specimens of 22 mm × 1.5 m

increase in the impact momentum. However, this tendency needs to be confirmed in the future since both the number of specimens which failed in the tests and the range of the destructive impact momentum were too small.

4.4 Diameter Reduction

Three specimens, M6, M7 and M8, tested by an impact of 50 kJ, did not fail after the first drop. The steel tubes of the specimens were cut open after testing, and the diameters of the bolt shank were measured. The measurement data are presented in Fig. 10. The original diameter of the bolt shank was 21.9 mm. The diameter of the specimens was evenly reduced along the entire length of the stretch section from its original value of 21.9 to 20.5 mm.

4.5 Dynamic Displacement

The ultimate displacements of the bolt sections are presented in Table 2. The average ultimate strain of the specimens obtained is approximately 16–17%. The deformation characteristics of a few pieces of dynamic and static test specimens were studied in detail with regard to the diameter changes of their shanks. The average diameters of four dynamically tested specimens and three statically tested specimens are presented in Fig. 11. It is seen that the decrease in diameter of the dynamic test specimens is more pronounced than that of the static test specimens. This proves that the bolt shank elongates more under dynamic loading than under static loading. This indicates that the dynamic deformation capacity of a bolt is slightly larger than its static deformation capacity.

It is well known in material science that materials like steel become more brittle when subjected to a high-strain loading rate (>100 μ strains). This implies that the material deforms less under dynamic loading than under static loading. The test results in this study do not show this tendency.

Table 2 Ultimate displacements of bolt sections under dynamic loading

| Specimen | Section length (mm) | Ultimate displ. (mm) | Ultimate strain ^a (%) |
|----------|---------------------|----------------------|----------------------------------|
| M2 | 1,500 | 234 | 17 |
| M3 | 1,500 | 236 | 17 |
| M4 | 1,500 | 226 | 16 |
| M5 | 1,500 | 225 | 16 |
| D2-A3 | 800 | 142 | 18 |
| D2-A6 | 800 | 143 | 18 |

Effective stretch length = test section length – one anchor length (100 mm)

^a The ultimate strain is calculated using the effective stretch length

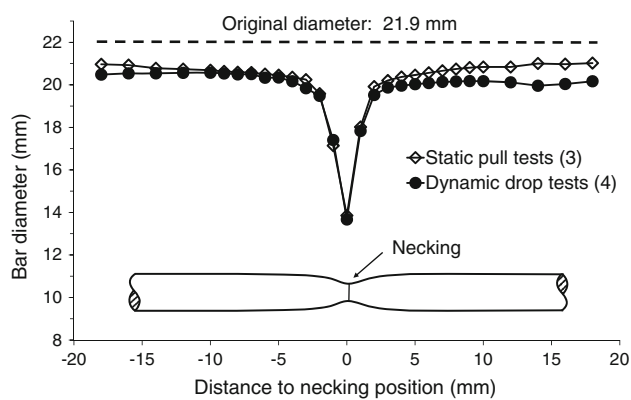


Fig. 11 Diameter variation of static and dynamic bolt specimens after the failure of the bolt shank

One explanation for the discrepancy may be that the loading rate used in this study is too low to be counted as high-strain rate. The loading rate used in the study has not caused changes in the deformation behaviour of the steel. The increase in the dynamic ultimate displacement may be explained from the viewpoint of a time delay in the initiation of necking failure. It may take a longer time to initiate necking failure under dynamic loading than under static loading. The delay of the necking failure would result in the bolt shank having a longer time to elongate so that a larger displacement would occur to the end under dynamic loading.

4.6 Comparison with Some Other Yielding Rock Bolts

The dynamic test results of two D-bolt sections are presented in Fig. 12 together with the results of cone bolts and threadbars. All the data except those for the D-bolt sections are taken from a presentation by Cai and Champaigne (2010). Both the D-bolt and the threadbar absorb energy through plastic elongation of the bolt steel. The dashed line describes the relationship between the displacement and the impact energy for this category of rock bolt. Cone bolts

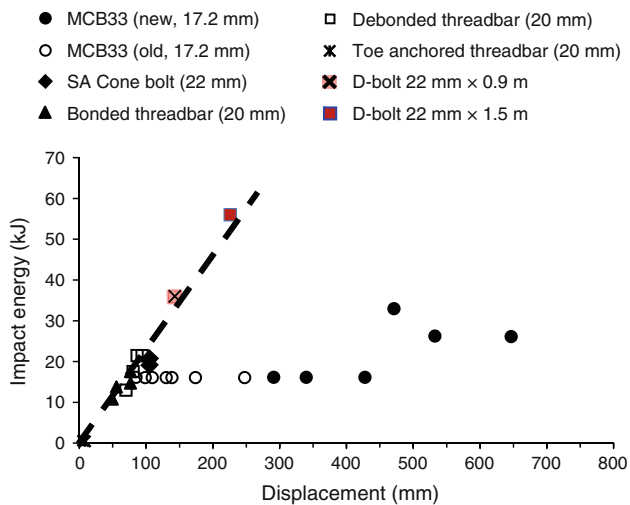


Fig. 12 Energy absorption versus displacement for different types of rock bolts. All data except those of the D-bolt sections are redrawn from Cai and Champaigne (2010)

absorb energy through ploughing of the cone in the grout. These two categories of bolts are different in the sense that they need different displacements to absorb a given amount of energy. For instance, a 1.5-m-long D-bolt section absorbs 50 kJ of energy after an elongation of about 0.2 m, while a cone bolt needs to displace by 0.5–0.75 m to absorb 30–33 kJ of energy. Notably, displacement is a quantity which should be restrained by the support system rather than to which the support system should adapt. To absorb a given amount of energy, the smaller the displacement of the bolt is, the better the support effect is. Thus, the energy absorption per unit displacement is an appropriate parameter to evaluate the performance of a rock bolt. In this sense, the D-bolt has a good dynamic performance since it absorbs a large amount of energy only after a limited amount of displacement.

5 Conclusions

The displacement of the D-bolt is linearly related to the impact energy ($mv^2/2$) when it is subjected to a dynamic load. Its energy absorption is proportionally related to the volume of the bolt section as well as the tensile strength and ultimate strain of the bolt material. The dynamic tests presented herein show that a D-bolt section with dimensions of 22 mm \times 1.5 m can sustain an impact of 56 kJ and absorb 60 kJ of energy prior to failure. The maximum impact energy of the 22 mm bolt is thus 37 kJ per metre of bolt and the maximum energy absorption is 40 kJ/m.

The impact energy determines whether the bolt will fail or not, while the momentum (mv) determines the impact

duration. The impact duration increases linearly with an increase in momentum as long as the bolt shank holds. However, it decreases with momentum if the dynamic energy is so large that the bolt shank fails after the strike. In other words, the impact duration becomes shorter with an increase in momentum in the case of bolt failure.

The bolt shank elongates uniformly along its length. Both the longitudinal elongation and radial reduction of the shank are identical along the entire length of the loaded bolt section.

The ultimate dynamic displacement of the bolt is 16–17% of the bolt length. The bolt can elongate slightly more under dynamic loading than under static loading. This displacement increase may be attributed to the delay in necking failure when the bolt shank is subjected to dynamic loading.

Acknowledgments The authors would like to thank Xstrata Nickel, Canada, for its support for some of the tests. The authors are also grateful to Dr. Graham Swan for constructive discussions in the early stages of this work and to Mr. Ted Anderson, CANMET-MMSL, Canada, for his enthusiastic engagement and professional laboratory work.

References

- Cai M, Champaigne D (2010) Development of a fully debonded cone bolt for rockburst support. In: Jan MVS, Potvin Y (eds) Deep mining 2010. In: Proceedings of the 5th international seminar deep and high stress mining, 6–8 Oct 2010, Santiago, Chile. Australian Centre for Geomechanics, pp 392–342
- CAMIRO (1995) Canadian rockburst research program 1990–1995—a comprehensive summary of five years of collaborative research on rockbursting in hard rock mines. CAMIRO Mining Division, Canada
- Charette F, Plouffe M (2007) Roofex—results of laboratory testing of a new concept of yieldable tendon. In: Potvin Y (ed) Deep mining 07. In: Proceedings of the 4th international seminar deep and high stress mining. Australian Centre for Geomechanics, Perth, pp 395–404
- Jager AJ (1992) Two new support units for the control of rockburst damage. In: Kaiser PK, McCreath DR (eds) Proceedings of the international symposium rock support. Balkema, Rotterdam, pp 621–631
- Li CC (2010) A new energy-absorbing bolt for rock support in high stress rock masses. *Int J Rock Mech Min Sci* 47:396–404
- Li CC (2011a) Chapter 18. Rock support for underground excavations subjected to dynamic loads and failure. In: Zhou Y, Zhao J (eds) Advances in rock dynamics and applications. CRC Press, Taylor & Francis Group, Boca Rotan, pp 483–506
- Li CC (2011b) Performance of the D-bolt under static loading. *Rock Mech Rock Eng*. doi:10.1007/s00603-011-0198-6
- McCreath CD, Kaiser PK (1992) Evaluation of current support practices in burst-prone ground and preliminary guidelines for Canadian hardrock mines. In: Kaiser PK, McCreath DR (eds) Proceedings of the international symposium rock support. Balkema, Rotterdam, pp 611–619
- Ortlepp D (1992) Invited lecture: the design of support for the containment of rockburst damage in tunnels—an engineering approach. In: Kaiser PK, McCreath DR (eds) Proceedings of the

- international symposium rock support, Sudbury, ON, Canada, Balkema, pp 593–609
- Ortlepp D (1994) Grouted rock-studs as rockburst support: a simple design approach and an effective test procedure. *J South Afr Inst Min Metall* 94(2):4763
- Ortlepp D, Stacey TR (1995) Technical note: safety and cost implications in the spacing of support. *J South Afr Inst Min Metall*, pp 141–146
- Player J, Thompson A, Villaescusa E (2008) Dynamic testing of reinforcement systems. In: Stacey TR, Malan DF (eds) 6th international symposium ground support in mining and civil engineering construction, Cape Town, South Africa. SAMM symposium series S51, pp 597–622
- Simser B (2001) Geotechnical review of the July 29, 2001. West ore zone mass blast and the performance of the Brunswick/NTC rockburst support system. Tech Rep
- Varden R, Lachenicht R, Player J, Thompson A, Villaescusa E (2008) Development and implementation of the Garford Dynamic Bolt at the Kanowna Belle Mine. In: 10th underground operators' conference, Launceston, Australia
- Wu R, Oldsen J (2010) Development of a new yielding rock bolt—Yield-Lok bolt. In: The 44th US rock mechanics symposium, Salt Lake City, USA, ARMA, pp 10–197